Int. J. Electrochem. Sci., 11 **(2016)** 2638 - 2649

International Journal of
ELECTROCHEMICAL
SCIENCE
www.electrochemsci.org

Simultaneous Electrochemical Determination of Dopamine, Uric acid, Tryptophan on Electropolymerized Aminothiazole and Gold nanoparticles Modified Carbon nanotubes Modified Electrode

Cheng Yu Yang, Shen-Ming Chen[*] *, Selvakumar Palanisamy*

Electroanalysis and Bio electrochemistry Laboratory, Department of Chemical Engineering and Biotechnology, National Taipei University of Technology, No.1, Section 3, Chung-Hsiao East Road, Taipei 106, Taiwan (ROC)
[*]E-mail: smchen78@ms15.hinet.net

Received: 21 December 2015 / *Accepted:* 7 February 2015 / *Published:* 1 March 2015

In the present work, a multifunctional biosensor was developed for the simultaneous determination of dopamine (DA), uric acid (UA) and tryptophan (Try) using 2-amino-thiazole (AT)/gold nanoparticles (AuNPs) functionalized multiwalled carbon nanotubes (*f*-MWCNT) modified electrode. The *f*-MWCNT/AuNPs-AT composite modified glassy carbon electrode (GCE) was prepared by electrodeposition of AT and followed by electrodeposition of AuNPs and drop casting of *f*-MWCNT on GCE. The formation of the composite was confirmed by atomic force microscopy, scanning electron microscopy and electrochemical studies. The *f*-MWCNT/AuNPs-AT modified GCE exhibits good electrocatalytic ability for the simultaneous determination of DA, UA and Try. Cyclic voltammetry and linear sweep voltammetry were used for simultaneous and selective determination of DA, UA and Try. Moreover, the modified electrode also provides good sensitivity and selectivity for the determination of DA, UA and Try.

Keywords: Dopamine, uric acid, tryptophan, carbon nanotubes, gold nanoparticles, electrocatalysis, multifunctional biosensor.

1. INTRODUCTION

Biosensor has become one of the most important diagnostic tools in the industrial process control, environmental monitoring and different applications in medicine and biotechnology. However, the use of bare electrodes in such analysis has numerous limitations such as high overpotential, slow electron transfer, low sensitivity and selectivity and therefore chemically modified electrodes are developed to overcome these shortcomings [1–6]. Fabrications of highly sensitive and selective

biosensors represent the development and exploitation of analytical devices for detection, quantification and monitoring of specific chemical species in clinical, environmental and industrial analysis are highly desirable [7]. In recent years, different modified electrodes have been employed for determination of multi bio-compounds, for example, H_2O_2 and glucose can be easily detected by histidine/nickel hexacyanoferrate nanotube [8], carbon nanotube/chitosan/gold nanoparticles [9] and cobalt hexacyanoferrate nanoparticles/gold nanoparticles/multiwalled carbon nanotubes [10, 11]. Therefore, for many applications, it is necessary to fabricate an inexpensive multifunctional biosensor with redox active thin films for analytical applications of oxidation and reduction side.

Dopamine (DA), uric acid (UA) and tryptophan (Try) are usually coexist in human biological system and are important molecules for physiological processes in human metabolism. On the other hand, DA is one of the important neurotransmitter which plays vital role in the mammalian central nervous systems [12]. However, abnormal concentration of DA will leads to brain disorders such as Parkinson's disease and schizophrenia and therefore determination of DA is of great significance in the biological diagnoses [13, 14]. The electrochemical techniques are providing excellent platform for the detection of DA in biological diagnoses due to its simplicity, selectivity and sensitivity [15]. UA is one of the primary end products of purine metabolism; however, abnormal concentrations of UA are indications of several diseases such as hyperuricemia, gout, and Lesch-Nyan disease and hence determination of UA is highly important [16]. Tryptophan (Try) is one of the essential amino acid required in human for the production of hormones, neurotransmitters and other biomolecules. However, its concentration is crucial; abnormal concentrations of Try leading to hepatic disease [17]. At bare electrodes, the electrochemical signals of DA, UA and Try are often associated very close and overlaps which making their discrimination highly difficult [23 — 24]. In the literature, some modified electrodes are reported for the simultaneous determination of DA, UA and Try [18—22]. In the present work, a novel and stable functionalized multiwalled carbon nanotubes (*f*-MWCNT)/gold nanoparticles (AuNPs)/2-Amino-thiazole (AT) modified electrode was successfully prepared and used for the simultaneous determination of DA, UA and Try. The main aim of the present work is to prepare multifunctional sensor for the sensitive and selective determination of DA, UA and Try. The *f*-MWCNT/AuNPs-AT composite modified electrode was prepared by electrodeposition of AT and followed by electrodeposition of AuNPs and drop casting of *f*-MWCNT on glassy carbon electrode (GCE). The electrocatalytic ability of *f*-MWCNT/AuNPs-AT composite modified electrode was studied for the oxidation of DA, UA and Try.

2. EXPERIMENTAL

2.1. Materials and methods

$KAuCl_4.3H_2O$ was purchased from Strem Chemicals (USA). AT and all the other chemicals were purchased from Sigma-Aldrich (USA). Double distilled deionized (DD) water was used to prepare all the solutions. 0.1 M H_2SO_4 was used as supporting electrolyte for the electrodeposition of AT and Au films. All the electrochemical experiments were carried out under nitrogen atmosphere.

The electrochemical experiments were performed using a CHI 410a potentiostat (CH Instruments, USA). The GCE with a diameter 0.3 cm from Bioanalytical Systems, Inc., USA was used for electrode modifications. A conventional three-electrode system which consisting of Ag/AgCl (saturated KCl) as a reference electrode, *f-MWCNT/AuNPs-AT modified GCE* as a working electrode and platinum wire as a counter electrode was employed for the electrochemical studies. Electrochemical impedance studies (EIS) were performed using a ZAHNER impedance analyzer (Germany). The atomic force microscope (AFM) images were recorded using a multimode scanning probe microscope (Being Nano-Instruments CSPM-4000, China). Scanning electron microscope (SEM) images were recorded using a HITACHI S-4700 (Japan).

2.2 Preparation of the modified electrode

Prior to the electrochemical deposition process, the GCE was well polished with aqueous slurries of alumina powder (0.05 μm) using a BAS polishing kit, then rinsed and ultrasonicated in DI water. As purchased MWCNT was hydrophobic in nature and could not produce a stable and homogeneous dispersion in aqueous media. The MWCNT was pre-treated and functionalized by following the procedures as reported early [25, 26]. Briefly, 150 mg of MWCNT was heated at 350ºC for 2 h and cooled to room temperature. Then, it was ultrasonicated for 4 h in concentrated HCl to remove impurities like amorphous carbon and metal catalysts. It was filtered and washed thoroughly with water until the pH was reached 7. The filtered MWCNT was dried at 100 ºC. The carboxylation of MWCNT was done by untrasonicating the pre-treated MWCNT in a mixture of sulfuric acid and nitric acid in 3:1 ratio for 6 h. It was then washed several times with water until the pH was neutral.

The electrochemical polymerization of AT film at GCE was carried out in 0.1 M H_2SO_4 containing 1 mM AT (inset to Fig. 2 (A'). The potential range was applied between - 1.5 to 2.0 V with scan rate of 0.1 V/s for 10 cycles. Then, AuNPs was electrodeposited in 0.1 M H_2SO_4 containing 1 mM $HAuCl_4.3H_2O$ at the potential ranges between - 0.5 V and 1.1 V with the scan rate of 0.1 V/s for 10 cycles (inset to Fig. 2 (B')). During the cycling process, a large anodic peak was observed at the potential of + 0.70 V corresponding to the reduction of Au^{3+} ions and nucleation of AuNPs on the electrode surface. After completion of the electropolymerization process, the electrode was dried in air oven for 5 min. Then, *f*-MWCNT was drop casted on AuNPs-AT modified GCE and dried to form the *f*-MWCNT/AuNPs-AT modified GCE. Finally, the *f*-MWCNT/AuNPs-AT modified GCE was treated by repeated electrochemical cycling at the potential range between – 0.2 and 1.0 V in 0.1 M phosphate buffer (pH 7.0). The control electrodes such as MWCNT/GCE, AuNPs/GCE, and AT/GCE were also prepared similar method as described above.

3. RESULT AND DISCUSSION

3.1 Surface morphological investigation of the f-MWCNT/AuNPs-AT film

The morphology of the different composites was studied by AFM and SEM. Fig. 1 shows the AFM images for (a) AT/ITO, (b) AuNPs/ITO, (c) *f*-MWCNT/ITO, and (d) *f*-MWCNT/AuNPs-

AT/ITO. The AFM image of AT/ITO presents the electrodeposited AT with very good porous surface required for the electrocatalysis, while the AFM image of AuNPs/ITO shows the typical particles like morphology of the gold nanoparticles.

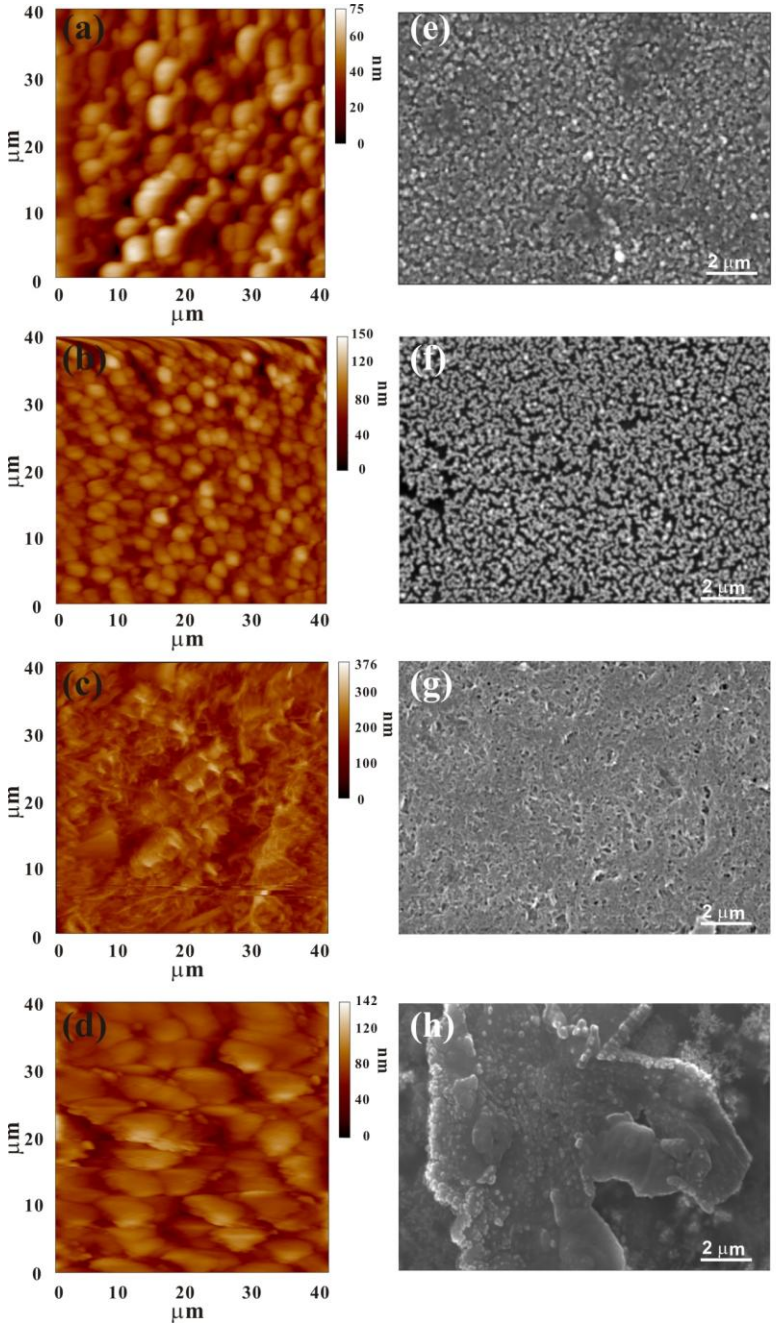

Figure 1. AFM images for (a) AT/ITO, (b) AuNPs/ITO, (c) *f*-MWCNT/ITO and (d) *f*-MWCNT/AuNPs-AT/ITO. The SEM images for (e) AT/ITO, (f) AuNPs/ITO, (g) *f*-MWCNT/ITO, and (h) *f*-MWCNT/AuNPs-AT/ITO.

AFM image of *f*-MWCNT/ITO depicts the characteristic MWCNT tubular morphology, while the AFM image of the *f*-MWCNT/AuNPs-AT/ITO shows the highly porous surface with more sites. The SEM images also presents the similar results observed in AFM studies. (AT/ITO (e), AuNPs/ITO

(f), *f*-MWCNT/ITO (g), and *f*-MWCNT/AuNPs-AT/ITO (h)). The AFM and SEM observations clearly revealed the successful formation of the *f*-MWCNT/AuNPs-AT composite.

3.2 Electrochemical properties of f-MWCNT/AuNPs-AT modified electrode

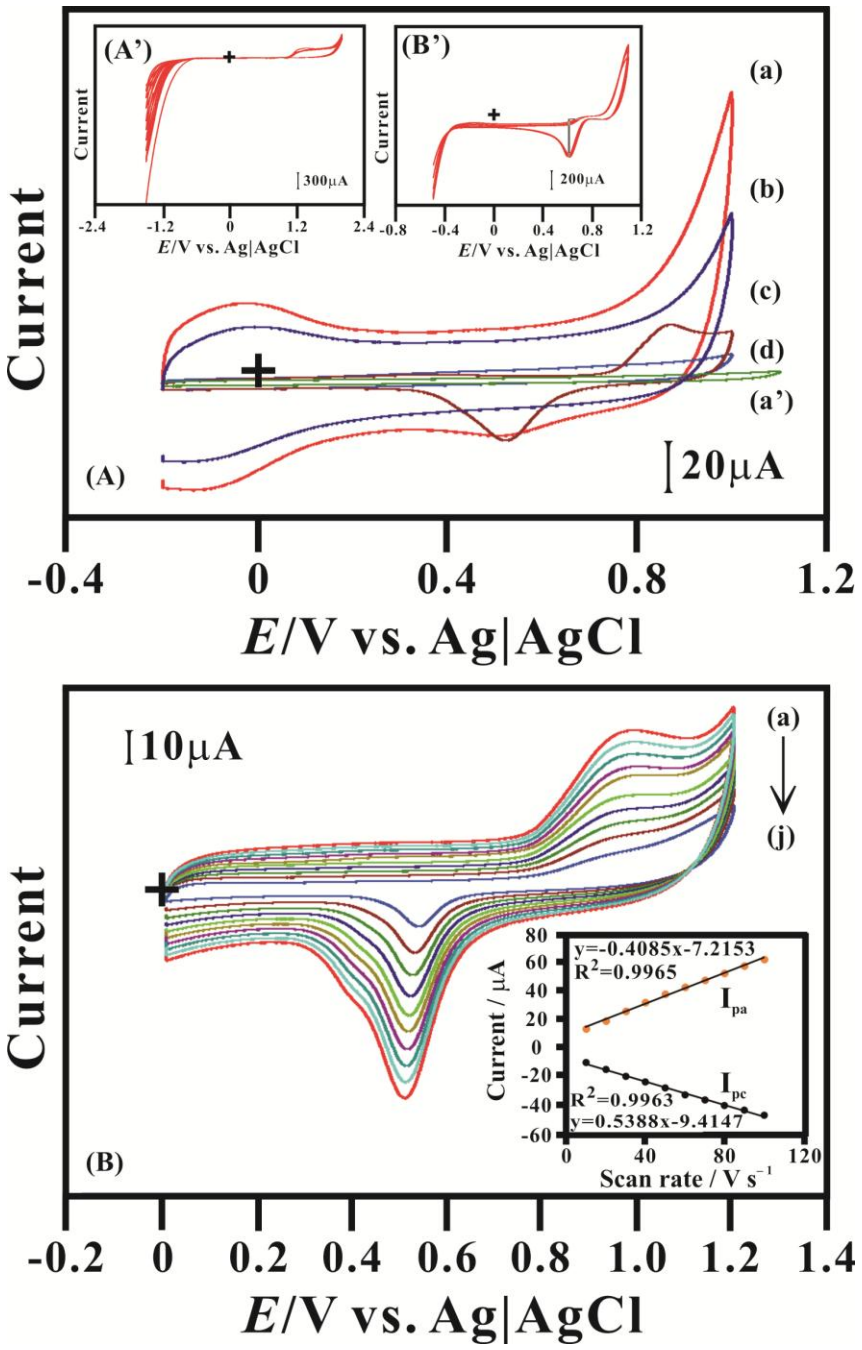

Figure 2. (A) Cyclic voltammograms obtained at (a) *f*-MWCNT/AuNPs-AT/GCE, (b) MWCNT/GCE, (c) Au/GCE, (d) AT/GCE and (a') bare GCE in 0.1 M phosphate buffer (pH 7). B) Cyclic voltammograms obtained at *f*-MWCNT/AuNPs-AT/GCE at various scan rates. Inset: scan rate vs. peak currents.

Fig. 2A shows the cyclic voltammograms obtained at (a) *f*-MWCNT/AuNPs-AT/GCE, (b) MWCNT/GCE, (c) AuNPs/GCE, (d) AT/GCE and (a') bare GCE in 0.1 M phosphate buffer (pH 7). The *f-MWCNT/AuNPs-AT/GCE* exhibits significantly improved and highly enhanced capacitive current in comparison with all other modified electrodes. Therefore, *f-MWCNT/AuNPs-AT/GCE* is highly capable to utilize in electrocatalytic applications. Fig. 2B exhibits the different scan rate studies of *f*-MWCNT/AuNPs-AT film modified GCE in the scan ranges of 10–100 mV/s (a–j). As expected, the cyclic voltammograms of *f*-MWCNT/AuNPs-AT/GCE exhibited anodic peaks at the potential of 1.0 V, and cathodic peak at 0.52 V. The anodic and cathodic peak currents linearly increase as the scan rate increases from 10 to 100 mV/s. The corresponding linear regression equations are, I_{pa} (μA) = 0.539 v (V/s) + 9.4147, R^2 = 0.9963 and I_{pc} (μA) = – 0.4085 v (V/s) – 7.215, R^2 = 0.996. The result indicates that the electron transfer process involves a surface confined species and the charge transfer is fast in the coating [35].

3.3 pH effect and EIS analysis

The electrochemical behavior of the *f*-MWCNT/AuNPs-AT/GCE was investigated under different pH conditions (a) pH 1, (b) pH 3, (c) pH 5, (d) pH 7, (e) pH 9, (f) pH 11 and (g) pH 13) (Fig. 3A). As shown in the figure, the voltammograms obtained at different pH values are different. The formal potential ($E^{0'}$) of the redox couple was shifted to more negative potential direction and peak currents decreases with increasing pH value. The plot of $E^{0'}$ versus pH exhibits good linearity slope of - 63 mV pH^{-1} (inset of Fig. 3A). This result is very close to the Nernstian value of -59 mV pH^{-1} for a reversible process involved with equal numbers of electrons and protons. The pH dependence suggests that the electroactive sites on the *f-MWCNT/AuNPs-AT/GCE* behave as true surface active groups influenced by specific solution conditions and not shielded within the electrode interior. The electrode surface modification with f-MWCNT/AuNPs-AT, MWCNT, AuNPs, and AT that greatly changes the double layer capacitance and interfacial electron transfer resistance of the electrode.

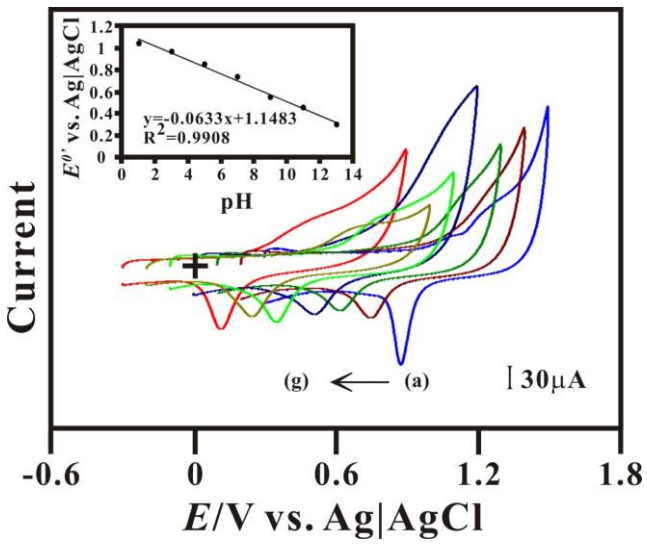

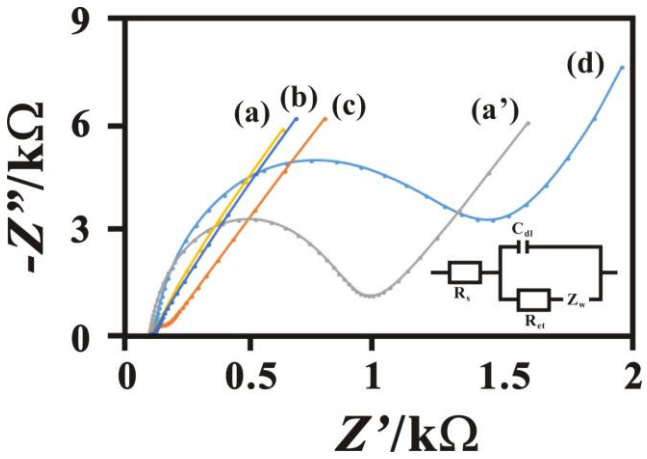

Figure 3. (A) Cyclic voltammograms obtained at (a) *f-MWCNT/AuNPs-AT/GCE*, (b) MWCNT/GCE, (c) Au/GCE, (d) AT/GCE and (a') bare GCE in 0.1 M phosphate buffer (pH 7). B) EIS of (a) *f*-MWCNT/ AuNPs -AT/GCE, (b) CNT/GCE, (c) AuNPs /GCE, (d) AT/GCE and (a') bare GCE in phosphate buffer (pH 7.0) containing 5 mM $K_3[Fe(CN)_6]/K_4[Fe(CN)_6]$

EIS can reveal the interfacial changes due to the surface modification of electrodes. Fig. 3B presents the EIS measurements of the modified electrodes represented as Nyquist plots for (a) *f*-MWCNT/AuNPs-AT/GCE, (b) MWCNT/GCE, (c) AuNPs/GCE, (d) AT/GCE and (a') bare GCE in phosphate buffer (pH 7.0) containing 5 mM $K_3[Fe(CN)_6]/K_4[Fe(CN)_6]$. The semicircle of the Nyquist plot designates the parallel combination of electron transfer resistance (R_{et}) and double layer capacitance (C_{dl}), while the linear portion represents the diffusion limited process. As shown in the figure, all the electrodes exhibit semicircles with different diameter. As shown in figure, the *f*-MWCNT/AuNPs-AT/GCE exhibits the smallest semicircle (R_{et} = 110 Ω) which clearly indicates the lower electron transfer resistance behavior in comparison with AuNPs/GCE (R_{et} = 160 Ω), *f*-MWCNT/GCE (R_{et} = 125 Ω), AT/GCE (R_{et} = 1300 Ω) and bare GCE (850 KΩ). Therefore, the EIS results revealed the excellent conducting property of the described modified electrode with might be due to the synergy between MWCNT, AuNPs and AT.

3.4 Electrocatalytic oxidation of DA, UA and Try with f-MWCNT/AuNPs-AT Film

The electrocatalytic oxidation of DA, UA and Try mixture is studied by cyclic voltammetry and compared with *f*-MWCNT/AuNPs-AT/GCE in the phosphate buffer. Fig. 4(a) to (c) presents the electrocatalytic oxidation of DA, UA, and Try respectively. In the presence of DA, a pair of quasi reversible redox couple with highly enhances peak currents for DA at the *f-MWCNT/AuNPs-AT/GCE*; however, bare GCE exhibits very poor electrocatalytic ability for DA. Here the anodic peak is due to the oxidation of DA to *o*-dopaminequinone, while the cathodic peak is due to the reduction of *o*-dopaminequinone to DA. Similarly, the *f*-MWCNT/AuNPs-AT/GCE shows significantly improved electrocatalytic ability to the electrocatalysis of UA and Try than that of bare GCE. The highly enhanced peak currents observed at *f*-MWCNT/AuNPs-AT/GCE indicates fast electron transfer kinetics and promising electrocatalytic ability of the modified electrode. Simultaneous determination

of DA, UA and Try was carried out at *f*-MWCNT/AuNPs-AT film and represented as Fig. 4(d). As shown in figure, the *f*-MWCNT/AuNPs-AT modified electrode exhibits well-defined three separate anodic peaks for DA, UA and Try.

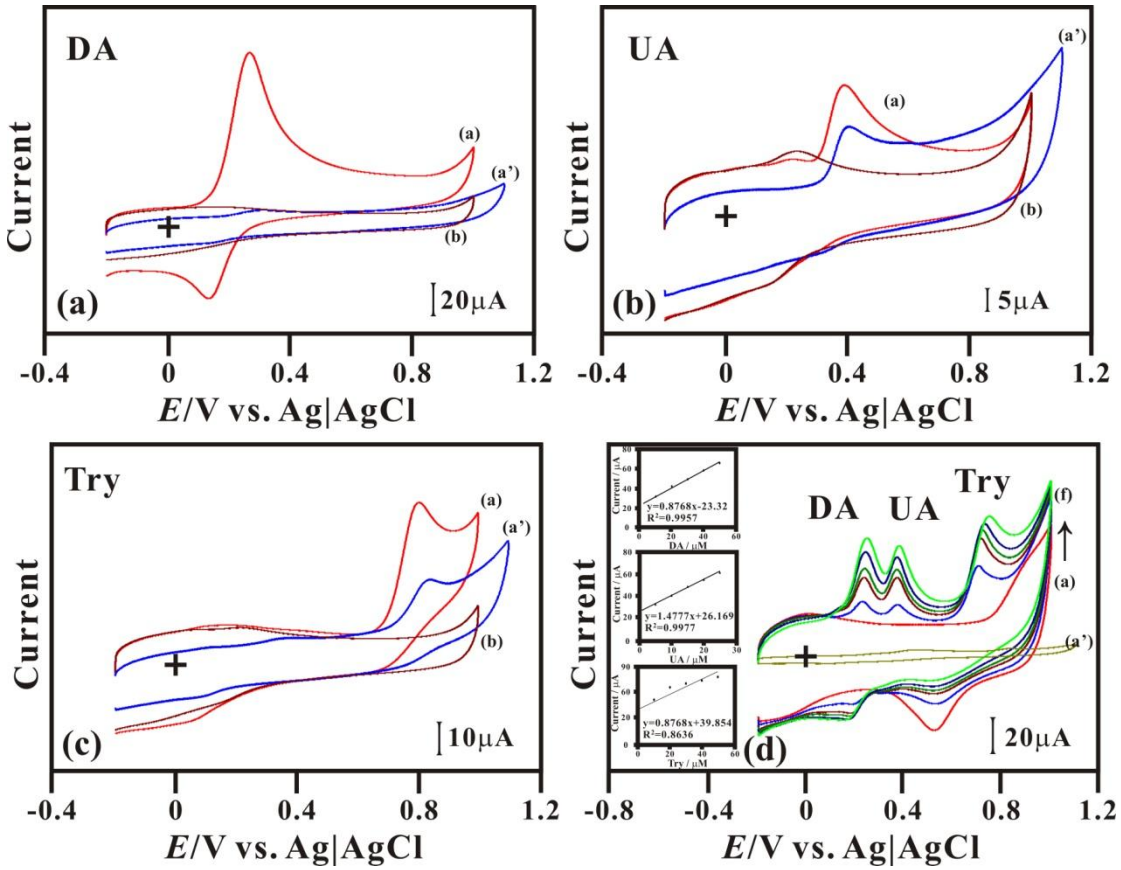

Figure 4. (a) Cyclic voltammograms obtained at *f*-MWCNT/AuNPs-AT in the absence (b) and presence of DA (a). Cyclic voltammograms obtained at bare GCE in the presence of DA (a'). (b) Cyclic voltammograms obtained at *f*-MWCNT/AuNPs-AT in the absence (b) and presence of UA (a). Cyclic voltammograms obtained at bare GCE in the presence of UA (a'). (c) Cyclic voltammograms obtained at *f*-MWCNT/AuNPs-AT in the absence (b) and presence of Try (a). Cyclic voltammograms obtained at bare GCE in the presence of Try (a'). (d) Cyclic voltammograms obtained at *f*-MWCNT/AuNPs-AT in the presence of various concentrations of DA, UA and Try. Inset: calibration plots for DA, UA and Try.

Here the *f*-MWCNT/AuNPs-AT modified electrode resolves the mixed voltammetric response of DA, UA and Try into three well-defined voltammetric peaks at 0.24 V, 0.37 V and 0.72 V respectively. The peak separations between DA, UA and Try are sufficient enough to determine these species with good selectivity and sensitivity. The peak current increases linearly, as the concentrations of DA, UA and Try increases. The linear concentration range was obtained as 10–50 μM, 5–25 μM and 10–50 μM for DA, UA and Try, respectively. From the calibration plots, the linear regression equations for the simultaneous determination of DA, UA and Try at *f*-MWCNT/AuNPs-AT modified electrode were expressed as $I_{pa(DA)}$ (μA) =0.877 (μM) + 23.32, R^2=0.9957 with sensitivity of 13.53

$\mu A \mu M^{-1}$ cm^{-2}, $I_{pa(UA)}$ (μA) = 1.478 [UA] + 26.20, R^2=0.998 with the sensitivity of 21.1 $\mu A \mu M^{-1}$ cm^{-2} and $I_{pa(Try)}$ (μA) = 0.897 (μM) + 39.85, R^2 = 0.864 with sensitivity of 12.82 $\mu A \mu M^{-1}$ cm^{-2}.

Table. 1 Comparison of analytical performance of MWCNT/AuNPs-AT modified electrode with previously reported modified electrodes for determination of DA, UA and Try.

Electrode	DA		UA		Try		Ref.
	LOD (μM)	Linear range (μM)	LOD (μM)	Linear range (μM)	LOD (μM)	Linear range (μM)	
GNPs/PImox/GCE	0.08	up to 268.0	0.5	up to 486.0	0.7	up to 34.0	27
GS–PTCA/GCE	0.13	up to 374.0	0.92	up to 544.0	0.06	up to 138.0	28
Trp-GR/GCE	0.29	up to 110.0	1.24	up to 1000.0	–	–	29
MWNTs/MGF/GCE	0.06	up to 10.0	0.93	up to 100.0	0.87	up to 30.0	30
GNP/Ch/GCE	0.12	up to 80.0	0.6	up to 100.0	–	–	31
M-Meso-PANI/GCE	9.8	up to 300.0	5.3	up to 300.0	5.2	up to 300.0	32
AgNPs/rGO/GCE	5.4	up to 800.0	8.2	up to 800.0	7.5	up to 800.0	33
CPE	0.087	up to 900.0	15.0	up to 650.0	–	–	34
MWCNT/CPE	0.36	up to 100.0	0.27	up to 170.0	0.06	up to 100.0	35
MWCNT/AuNPs-AT/GCE	0.18	up to 50.0	1.6	up to 25.0	1.3	up to 50.0	**This work**

3.5 Determination of DA, UA and Try by linear sweep voltammetry

Fig. 5a shows the linear sweep voltammograms (LSVs) obtained at *f-MWCNT/AuNPs-AT/GCE* in increasing concentrations DA with fixed concentration of UA and Try in phosphate buffer (pH 7.0). The LSV peak corresponding to the oxidation of DA was found linearly increased in consonance with the increase in the concentration of DA. The coexisted UA and Try have no interference to the oxidation peak current of the DA indicating the selectivity of the DA detection even in the presence of UA and Try.

The inset of Fig. 5 (a) shows that the linear calibration plot for DA detection which expressed as $I_{pa(DA)}$ (μA) = 0.9752 (μM) + 140.12, R^2=0.996. Fig. 5 (b) shows the LSVs of *f-MWCNT/AuNPs-AT/GCE* in the presence of various concentrations of UA and fixed concentration of DA and Try (5 μM) in phosphate buffer (pH 7.0). The LSV peak corresponding to the oxidation of UA was found linearly increased as the concentration of UA. The coexisted DA and Try have no interference to the oxidation of UA. The inset of Fig. 5 (b) shows that the linear calibration plot for DA detection which expressed as $I_{pa(UA)}$ (μA) = 1.249 (μM) + 47.65, R^2=0.975. Similarly, the LSVs obtained for Try in the presence of DA and UA indicating that the presence of DA and UA has no influence on the peak currents of Try. Fig.5 (d) shows the simultaneous determination of DA, UA and Try with linear concentrations ranges of 5 to 30 μM, 20 to 120 μM and 50 to 300 μM respectively. The limit of detection (LOD) was calculated for DA, UA and Try as 0.18 μM, 1.6 μM and 1.3 μM, respectively. The analytical performance of the MWCNT/AuNPs-AT modified electrode was compared with previously reported modified electrodes for the determination of DA, UA and Try and the results are shown in Table. 1. It can be seen from the Table. 1 that the analytical performance (sensitivity, LOD

and linear response range) of the modified electrode is comparable with previously reported modified electrodes for determination of DA, UA and Try [27–35]. Hence, MWCNT/AuNPs-AT modified electrode can be used for sensitive detection of DA, UA and Try.

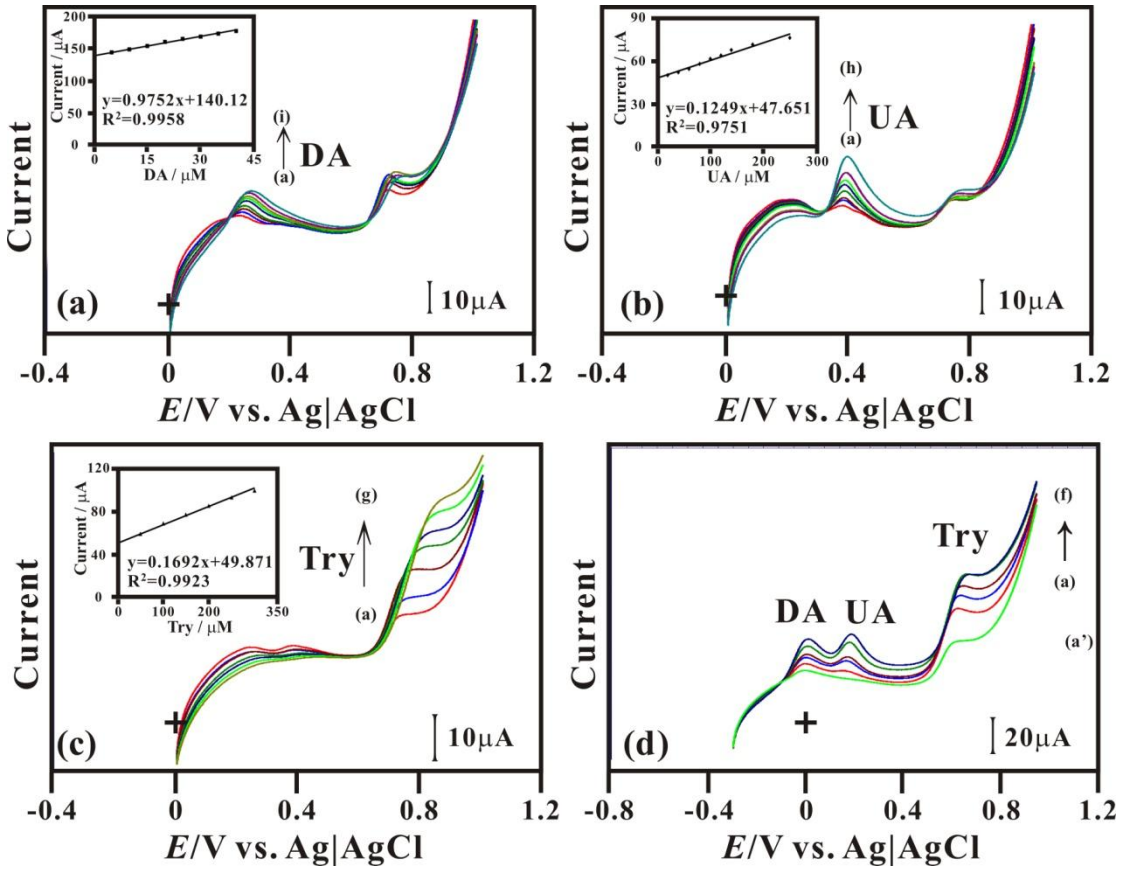

Figure 5. (a) LSVs obtained at *f-MWCNT/AuNPs-AT/GCE* in phosphate buffer (pH 7.0) at different concentrations of DA (a to i) containing fixed concentrations of UA and Try (5 μM). Inset: [DA] vs. response current. (b) LSVs obtained at *f-MWCNT/AuNPs-AT/GCE* in phosphate buffer (pH 7.0) at different concentrations of UA (a to h) containing fixed concentrations of DA and Try (5 μM). Inset: [UA] vs. response current. (c) LSVs obtained at *f-MWCNT/AuNPs-AT/GCE* in phosphate buffer (pH 7.0) at different concentrations of Try (a to g) containing fixed concentrations of DA and UA (5 μM). Inset: [Try] vs. response current. (d) LSVs obtained at *f-MWCNT/AuNPs-AT/GCE* in phosphate buffer (pH 7.0) at different concentrations of DA, UA and Try (a to f).

3.6. Determination of DA, UA and Try in human real samples

The MWCNT/AuNPs-AT modified electrode was further used for the determination of DA, UA and Try in real samples. For this, we have used LSV for the determination of DA, UA and Try in human serum samples using the standard addition method [36–38]. The experimental conditions are same as of in Fig. 4. The recovery of DA, UA and Try in human serum samples were tabulated in Table. 2. The average recovery of DA, UA and Try in human serum samples were found as 97.9, 97.7

and 97.0%, respectively. The result validates that the MWCNT/AuNPs-AT modified electrode has appropriate recovery towards the determination of DA, UA and Try in human serum samples.

Table 2 Determination of DA, UA and Try in human blood serum samples at MWCNT/AuNPs-AT modified electrode by LSV.

Sample	**Added (μM)**			**Found (μM)**			**Recovery (%)**		
	DA	UA	Try	DA	UA	Try	DA	UA	Try
Human blood serum	–	–	–	–	–	–	–	–	–
	20.0	–	–	19.6	–	–	98.0	–	–
	20.0	50.0	–	39.4	48.8	–	98.5	97.6	–
	20.0	50.0	30.0	58.3	97.8	29.1	97.2	97.8	97.0

4. CONCLUSIONS

In summary, a multifunctional biosensor was developed for the simultaneous determination of DA, UA and Try at *f*-MWCNT/AuNPs-AT/GCE. The film was prepared by electrodeposition of AT and AuNPs and drop casting of *f*-MWCNT on GCE. The successful formation of the respective film was confirmed by atomic force microscopy, scanning electron microscopy and electrochemical studies. The *f*-MWCNT/AuNPs-AT/GCE exhibits excellent electrocatalytic ability for the simultaneous determination of DA, UA and Try. A multifunctional biosensor was fabricated for the sensitive and selective determination of DA, UA and Try by cyclic voltammetry and LSV. As a future perspective, *f*-MWCNT/AuNPs-AT composite can be used for simultaneous and selective detection of DA, UA and Try.

ACKNOWLEDGEMENT
This work was supported by the National Science Council and the Ministry of Education of Taiwan (Republic of China).

References

1. R.W. Murray, in Bard, A.J. (Ed.), *Electroanal. Chem.*, Marcel Dekker, New York, 1983.
2. A.E. Gorshteyn, A. Robbat, Jr., *Ind. Eng. Chem. Res*., 39 (2000) 2006.
3. L.J.J. Janssen, L. Koene, *Chem. Eng. J*., 85 (2002) 137.
4. K.S. Yun, J. Gil, J. Kim, H.J. Kim, K. Kim, D. Park, M. Kim, H. Shin, K. Lee, J. Kwak, E. Yoon, *Sens. Actuators* B, 102 (2004) 27.
5. J. Wang, *Trends Anal. Chem*., 21 (2002) 226.
6. Y. Torisawa, N. Ohara, K. Nagamine, S. Kasai, T. Yasukawa, H. Shiku, T. Matsue, *Anal. Chem.*, 78 (2006) 7625.
7. M. Albareda-Sirvent, A. Merkoci, S. Alegret, *Sens. Actuators B*, 69 (2000) 153.
8. M. Yang, J. Jiang, Y. Lu, Y. He, G. Shen, R. Yu, *Biomaterials*, 28 (2007) 3408.

9. Y. Wang, W. Wei, X. Liu, X. Zeng, *Mater. Sci. Eng., C* C 29 (2009) 50.
10. S. Wang, L. Lu, M. Yang, Y. Lei, G. Shen, R. Yu, *Anal. Chim. Acta,* 651 (2009) 220.
11. K.C. Lin, T.H. Tsai, S.M. Chen, *Biosens. Bioelectron.,* 26 (2010) 608.
12. C. Xue, Q. Han, Y. Wang, J. Wu, T. Wen, R. Wang, J. Hong, X. Zhou, H. Jiang, *Biosens. Bioelectron.,* 49 (2013) 199.
13. Y. Wang, Y. Li, L. Tang, J. Lu, J. Li, *Electrochem. Commun.,* 11 (2009) 889.
14. R. Devasenathipathy, V. Mani, S.-M. Chen, B. Viswanath, V. Vasantha, M. Govindasamy, *RSC Adv.*, 4 (2014) 55900.
15. V.K. Ponnusamy, V. Mani, S.-M. Chen, W.-T. Huang, J. Jen, *Talanta*, 120 (2014) 148.
16. S. Thiagarajan, S.-M. Chen, *Talanta*, 74 (2007) 212.
17. X. Tang, Y. Liu, H. Hou, T. You, *Talanta*, 80 (2010) 2182.
18. S. Thiagarajan, T.H. Tsai, S.M. Chen, *Biosens. Bioelectron*., 24 (2009) 2712.
19. H.R. Zare, N. Nasirizadeh, M. Mazloum-Ardakani, *J. Electroanal. Chem*., 577 (2005) 25.
20. A.Balamurugan, S.M. Chen, *Anal. Chim. Acta*, 596 (2007) 92.
21. J. Mathiyarasu, S. Senthilkumar, K.L.N. Phani, V. Yegnaraman, *Mater. Letters*, 62 (2008) 571.
22. S. Harish, J. Mathiyarasu, K.L.N. Phani, V. Yegnaraman, *J. Appl. Electrochem*., 38 (2008) 1583.
23. T.H. Tsai, T.W. Chen, S.M. Chen, *Electroanalysis*, 22 (2010) 1655.
24. H. Elzanowska, E. Abu-Irhayem, B. Skrzynecka, V. I. Birss, *Electroanalysis*, 16 (2004) 478.
25. S. Jeykumari, D. R. Ramaprabhu and S. Narayanan, *Carbon*, 45 (2007) 1340.
26. H. Su, R. Yuan, Y. Chai, Y. Zhuo, C. Hong, Z. Liu and X. Yang, *Electrochim. Acta*, 54 (2009) 4149.
27. C. Wang, R. Yuan, Y. Chai, S. Chen, F. Hu, M. Zhang, *Anal. Chim. Acta*, 741 (2012) 15.
28. W. Zhang, Y. Chai, R. Yuan, S.Chen, J. Han, D. Yuan, *Anal. Chim. Acta*, 756 (2012) 7.
29. Q. Lian, Z. He, Q. He, A. Luo, K. Yan, D. Zhang, X. Lu, X. Zhou, *Anal. Chim. Acta*, 823 (2014) 32.
30. H. Li, Y. Wang, D. Ye, J. Luo, B. Su, S. Zhang, J. Kong, *Talanta*, 127(2014) 255.
31. P. Wang, Y. Li, X. Huang, L. Wang, *Talanta*, 73 (2007) 431.
32. M.U. Anu Prathap, R. Srivastava, *Sens. Actuators B*, 177 (2013) 239.
33. B. Kaur, T. Pandiyan, B. Satpati, R. Srivastava, *Colloids Surf., B* 111 (2013) 97.
34. M. Mazloum-Ardakani, H. Beitollahi, B. Ganjipour, H. Naeimi, M. Nejati, *Bioelectrochemistry*, 75 (2009) 1.
35. S.M. Ghoreishi, M.Behpour, F.. Ghoreishi, S. Mousavi, *Arabian J. Chem.*, (2013), http://dx.doi.org/10.1016/j.arabjc.2013.05.016.
36. B. Thirumalraj, S. Palanisamy, S.M. Chen, *Int. J. Electrochem. Sci.*, 10 (2015) 4173.
37. S. Palanisamy, S. Sakthinathan, S.M. Chen, B. Thirumalraj, T.H. Wu, B.S. Lou, X. Liu, *Carbohydr. Polym.*, 135 (2016) 267.
38. B. Thirumalraj, S. Palanisamy, S.M. Chen, B.S. Lou, *J. Colloid Interface Sci.*, 462 (2016) 375.